Low-frequency sheath instability stimulated by an energetic ion component

Mikhail Starodubtsev[a)]
Institute of Applied Physics, Nizhny Novgorod 603950, Russia

Md. Kamal-Al-Hassan, Hiroaki Ito, Noboru Yugami, and Yasushi Nishida
Energy and Environmental Science, Graduate School of Engineering, Utsunomiya University, 7-1-2 Yoto, Utsunomiya Tochigi 321-8585, Japan

(Received 27 July 2005; accepted 29 November 2005; published online 17 January 2006)

Spontaneous low-frequency oscillations have been observed in the circuit of a positively biased electrode immersed in a non-Maxwellian laboratory plasma containing an energetic ion component produced by the resonant absorption of a short microwave pulse in a nonuniform plasma column. The oscillations are found to be due to an instability of the electron-rich sheath. The instability with its characteristic frequency below the ion plasma frequency is driven by the energetic ion component reflected in the sheath area. A qualitative model of the instability is suggested.
 [DOI: 10.1063/1.2158697]

I. INTRODUCTION

Although the properties of plasma sheaths have been investigated since the first laboratory plasma experiments,[1] they are still the subject of numerous studies, both theoretical[2–5] and experimental.[6–10] This deep interest to sheath processes is stimulated mainly by their great importance for every device used in fundamental and applied plasma studies, such as plasma diagnostic techniques,[11–14] plasma diodes[15] and discharges,[2,9,16–18] antennas in plasmas,[6,7,13,19] current systems in space,[20–23] and satellite charging processes.[23–25]

High-frequency sheath-plasma processes, which occur in the vicinity of the local plasma frequency, have been widely studied in laboratory experiments.[6,7,13] Thus, the high-frequency sheath instability has been observed at the sheath-plasma antiresonance frequency, $\omega \approx \omega_p$ (ω_p is the plasma frequency), of a positively biased electrode;[6] the nature of the instability is connected with the finite electron transit time through the sheath. On the other hand, the sheath-plasma series resonance[13] has been observed as a narrow resonant enhancement in the shot noise below the plasma frequency.[7]

Low-frequency sheath processes have drawn considerable attention in the past decades.[6,8–10] Such processes can significantly affect the characteristics of probes,[6,8,10,12] discharges,[2,9] etc. A well-known feature of current overshoot in pulsed probe measurements[12] is observed near the plasma potential for positive voltage pulses and is caused by the inertia of ions in the sheath; similar time-dependent probe measurements in a large magnetoplasma[6] exhibit not only current overshoots but also low-frequency relaxation oscillations due to the current-driven instability. Low-frequency instability of a hollow-cathode discharge effecting the collapse of the cathode sheath voltage has been observed[9] and used to develop a new sort of high-power pulsed rf generators.[18] Spontaneous low-frequency dynatron oscillations caused by secondary electron emission have been detected, when an energetic electron beam is incident on an electrode.[8] Low-frequency noise excited by two counterstreaming ion flows has been found in the presheath of a negatively biased mesh probe.[10]

A new kind of low-frequency sheath instabilities has been recently observed[26] at the electron saturation current when a disk probe is immersed into the plasma perturbed by the resonant absorption of a microwave pulse. Basing on the characteristics of the observed instability, it has been assumed that the instability is stimulated by the energetic ion component produced during the resonant absorption of the microwave. It has been shown that this instability differs from the previously reported processes[2,6–10,12,13,17,18,21] and is characterized by the following features: (i) oscillations in the probe current occur only when the probe is biased positively with respect to the plasma potential, (ii) the instability is driven by a flux of suprathermal ions entering the sheath area of the probe, and (iii) the instability amplitude exhibits saturation, when the energetic ion component is reflected inside the sheath and cannot reach the probe surface.

The aim of the present paper is to describe the properties of this kind of low-frequency instabilities in more detail and to clarify the physics of the instability with new measurements.

Similar to our previous paper,[26] the high-energy ion component in the present experiment has been produced by resonant absorption of a short microwave pulse, whose duration is in the order of an ion plasma period. During this process, the incident electromagnetic wave is greatly enhanced in the region where its frequency is equal to the local plasma frequency.[27] This highly localized electric field produces a strong ponderomotive force which pushes plasma electrons down the field gradient. Accelerated electrons pull the ions by means of the ambipolar electric field[28] producing ion acceleration. As a result, an energetic ion component is found to propagate mainly downward the density gradient. Plasma density depletion, which arises in the resonant region, evolves as nonlinear ion waves propagating both upward and downward the density gradient. The above model

[a)]Electronic mail: mstar@appl.sci-nnov.ru

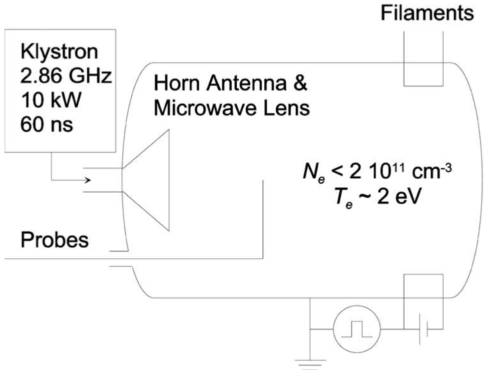

FIG. 1. Schematic view of the experimental setup.

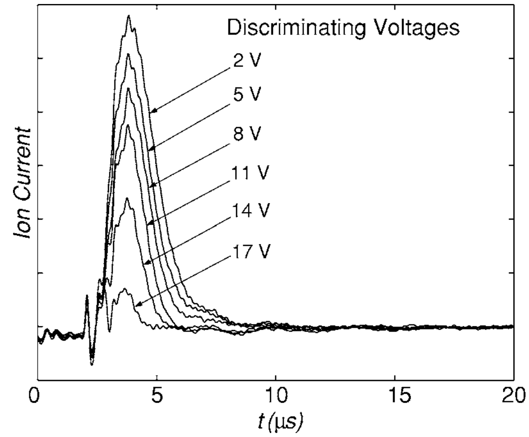

FIG. 2. Temporal behavior of ions accelerated toward the lower-density side measured with the energy analyzer at different potentials applied to the discriminating grid. The analyzer is located 3 cm below the resonant region.

is confirmed by our experimental observations but the exact identification of the ion acceleration process is beyond the scope of this paper.

The instability described hereafter may arise in different plasma applications, where a positively biased electrode interacts with a non-Maxwellian plasma containing a group of accelerated ions, such as tethered satellites incident by energetic ions inherently existing in space plasmas. Moreover, this instability may occur not only in the sheath of an electrode but also in plasma double layers, both in laboratory and space plasmas, if an energetic ion component enters into the double layer from the lower-potential side.[29,30]

II. EXPERIMENTAL SETUP

The experiments (see Fig. 1) are performed in a large (60 cm in diameter and 1 m in length) laboratory plasma device with a multipole magnetic confinement system. A nonuniform plasma column with a maximum density $n_e \approx 2 \times 10^{11}$ cm^{-3}, electron temperature $T_e \approx 2$ eV, and ion temperature $T_i \approx T_e/10$ is produced at the pressure of the argon gas $p = 4 \times 10^{-4}$ Torr with a pulsed dc discharge (pulse duration $\tau_{\text{dis}} = 2.5$ ms and repetition rate $f_{\text{dis}} = 10$ Hz) using a tungsten filament cathode. The typical density gradient scale lengths in the axial direction (z direction) and in the radial (r direction) are, respectively, $L_z = (\partial \ln n / \partial z)^{-1} \approx 100$ cm and $L_r = (\partial \ln n / \partial r)^{-1} \approx 50$ cm. A p-polarized microwave pulse with frequency $f = \omega / 2\pi = 2.86$ GHz and the maximum power of 10 kW is produced by a klystron and is radiated into the plasma volume from a high-gain horn antenna located at the lower-density side of the plasma chamber. The pulse width of the order of 60 ns at a full width at half maximum is approximately equal to the ion plasma period. The critical density layer ($\omega = \omega_p$, where ω_p is the plasma frequency) is located near the center of the chamber. Diagnostics used in the experiment include two oppositely directed disk probes measuring the ambient plasma density and its fluctuations, a microwave resonator probe,[31] a short dipole antenna, and an electrostatic energy analyzer oriented to the overdense plasma to measure the particles accelerated toward the lower-density side.

III. EXPERIMENTAL RESULTS

A. Energetic ion component

When the laboratory plasma is irradiated with a 10 kW, 60 ns pulse of a p-polarized microwave, high-amplitude, localized plasma oscillations are excited in the resonant region, where $\omega = \omega_p$. Nonlinear plasma-wave interaction occurring in this region produces strong plasma density disturbance, which reveals itself in two aspects. First, strong fluxes of energetic particles are ejected from the resonant region, mainly in the direction downward the density gradient.[28] A typical energy spectrum of the accelerated ion component observed in our experiments is displayed in Fig. 2 showing the presence of energetic ions with energies up to 17 V, which is approximately one order of magnitude larger than kT_e. These measurements were performed with an ion-energy analyzer, which discriminates against ions below a certain energy by a positive potential applied to the collector. Two grids are placed in front of the collector: the outer one is left at floating potential in order to reduce disturbances of the analyzer on the ambient plasma, while the inner one is biased negatively in order to reflect plasma electrons. The analyzer is located at approximately 3 cm down the density gradient from the resonant region. One can see that the resonant absorption of a short microwave pulse produces a group of accelerated ions with a wide range of ion velocities. As this ion structure travels down the density gradient, the peak disperses due to time-of-flight effect. As a result, a quiescent, Maxwellian plasma, which lies on the lower-density side of the plasma column, is penetrated by an energetic ion component.

Ejection of charged particles from the resonant region causes a density modification in this area. Two-dimensional (2D) plots displayed in Fig. 3 represent the evolution of plasma density after finishing the microwave pulse. Density perturbation occurred at the resonant layer during the conversion of resonant absorption into two short nonlinear ion acoustic waves propagating out of the resonant layer in the opposite directions: upward and downward the density gradient. The wave propagating downward the density gradient

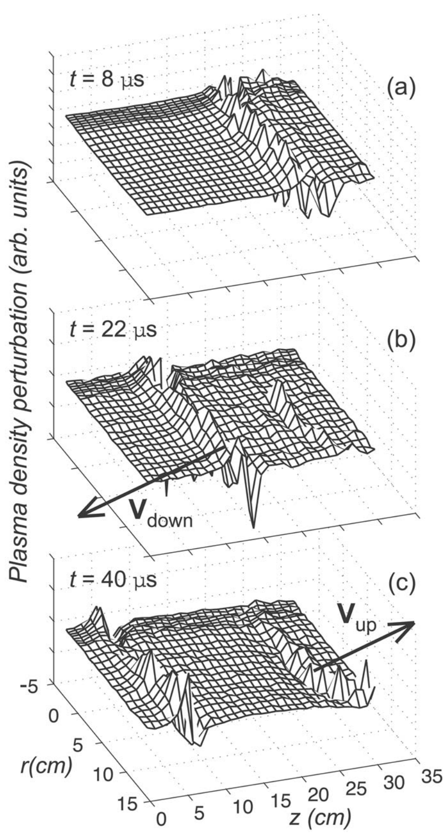

FIG. 3. Plasma density perturbation measured with a Langmuir probe (the ion saturation current). Strong modification of plasma density in the resonant region (a) gives rise to two ion waves propagating in opposite directions [(b) and (c)]. $V_{\rm down}\approx 2c_s$; $V_{\rm up}\approx c_s$.

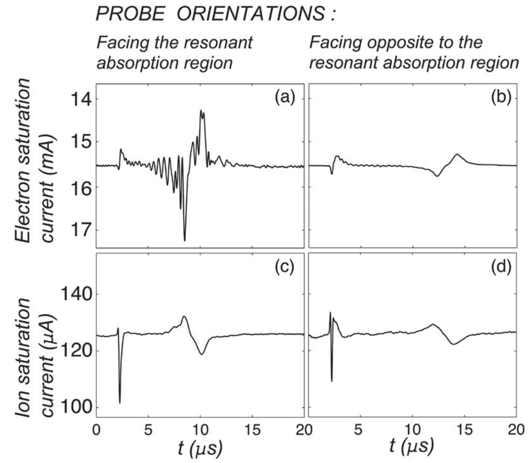

FIG. 4. Probe currents vs time at different probe orientations. [(a) and (b)] The electron saturation current (at $V=50$ V) when the probe facing the resonant absorption region (a) and facing opposite to the resonant absorption region (b). [(c) and (d)] The ion saturation current (at $V=-70$ V) when the probe facing the resonant absorption region (c) and facing opposite to the resonant absorption region (d). The probe is located 5 cm below the resonant region. Microwave pulse parameters: $P=10$ kW, $\tau=50$ ns.

is characterized by high amplitude (which may reach $0.1N_e$) and velocity $V_{\rm down}$ (which is approximately twice the ion acoustic speed c_s). The amplitude of the upward wave reaches only $0.03N_e$ and it propagates with $V_{\rm up}\approx c_s$.

B. Low-frequency sheath instability

Figure 4 shows a set of typical oscillograms of the electron and the ion saturation currents for two oppositely directed plane probes (both probes are 2 mm in diameter). The probes have been placed at the lower-density side of the resonant absorption region at a distance $\Delta z\approx 5$ cm from the resonance point (where $\Delta z=0$ corresponds to the resonant absorption point). In Figs. 4(b)–4(d), one can observe clearly the nonlinear ion wave propagating downward the density gradient. However, Fig. 4(a) displays not only the ion wave but also low-frequency oscillations with characteristic period $\tau_{\rm osc}\approx 0.3$ μs, which occur in the electron saturation current of a probe facing the resonance region. The aim of this paper is to uncover the nature of these oscillations. Different experimental tests have clearly shown that the observed low-frequency oscillations do not correspond to the real plasma density perturbations. We did not find any plasma parameter which may correlate with these oscillations. The fact that the oscillations observed in Fig. 4(a) do not correspond to the oscillating plasma density is evident, for example, from Figs. 4(b)–4(d), as the same phenomenon is not detected when the probe is biased in the ion saturation region [Fig. 4(c)], as well as by the probe facing opposite to the resonance region [Figs. 4(b)–4(d)]. Thus it is natural to suppose that the observed oscillations are due to an instability of the electron-rich sheath stimulated by a flux of energetic particles.

The nature of the oscillations has also been examined with a microwave resonator probe.[31] The probe design is shown in Fig. 5(a) and a set of oscillograms [Figs. 5(b)–5(e)] represents a comparison between the electron saturation currents (Figs. 5(b)–5(d), probe facing the resonant region) and the output signals of the resonator probe [Figs. 5(c)–5(e)]. A quarter-wavelength U-shaped high-quality ($Q\approx 170$) resonator exhibits a resonance at $f_{\rm res}\approx 4.88$ GHz in vacuum and $f^*_{\rm res}\approx 5.28$ GHz in plasma near the resonance region. Measurements were performed, when the signal frequency was tuned to the slope of the resonance curve ($f\approx 5.32$ GHz), such that small shifts of the resonant frequency due to plasma density perturbations produce approximately proportional variations of the amplitude of the probe output signal. The oscillograms from the resonator probe [Figs. 5(c)–5(e)] are similar to those presented in Figs. 4(b)–4(d) and do not display the oscillations observed in the electron saturation current [Figs. 5(b), 5(d), and 4(a)], although the probe time response is approximately $\tau\approx Q/f_{\rm res}\approx 30$ ns which is much shorter than the characteristic period of these oscillations.

The above results clearly demonstrate that the oscillations of the electron saturation current are not due to plasma density fluctuations but are related to the instability of the sheath. The formation of the instability is most evident when analyzing the normalized probe current $I_{\rm probe}/I_{\rm dc}$ (where $I_{\rm dc}$ is unperturbed probe current) as a function of the probe bias voltage V (Figs. 6 and 7). Figure 6 represents a set of normalized probe oscillograms from the probe facing the resonant region at different biases; Fig. 7 plots the relative instability amplitude (i.e., the ratio $I_{\rm osc}/I_{\rm dc}$) as functions of V. One may clearly observe that the instability occurs only when the probe is biased positively with respect to the plasma poten-

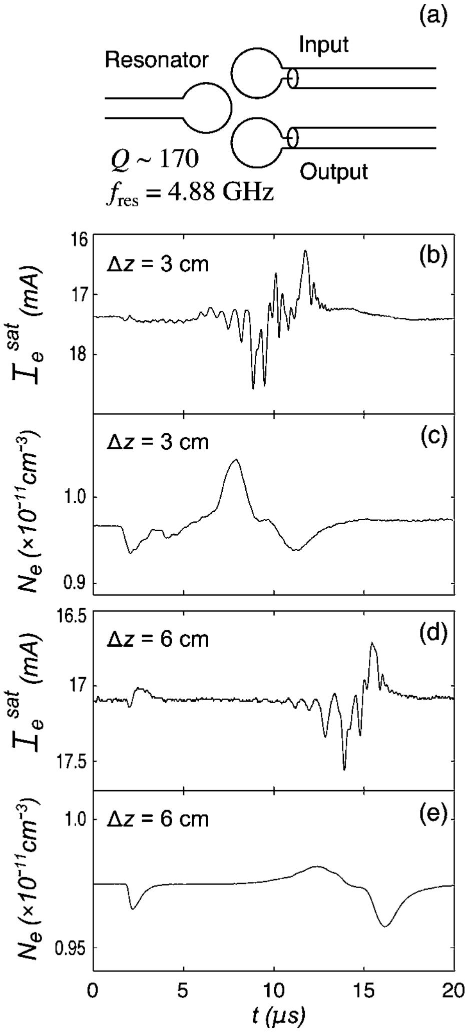

FIG. 5. Measurements of plasma density perturbations by using the microwave resonator probe. (a) Schematic view of the probe. [(b)–(d)] Comparison between the electron saturation currents [(b) and (d)] and the microwave probe output signals [(c) and (e)]. The latter are obtained at $f=5.32$ GHz and calibrated in terms of plasma density. Microwave probe parameters: resonance frequency in vacuum $f_{res}=4.88$ GHz, $Q\approx 170$. The probes are located 3 cm [(b) and (c)] and 6 cm [(d) and (e)] below the resonant region.

tial, which is indicated in Fig. 7 as V_{pl}. One can see that the relative amplitude of the observed oscillations does not remain constant (as it should be for the case of real density perturbations), but exhibits a threshold, growth, and saturation, i.e., typical behavior for instabilities.[32]

The instability has been observed only from the lower-density side of the resonant region, when an energetic flux of plasma particles produced by the resonant absorption process falls on the disk probe surface. The nature of the instability is related to the energetic ion flux, as it is evident from Fig. 8, which presents the temporal evolution of the electron saturation current at different distances Δz between the probe and the resonant region. One can see that the instability occurs before the nonlinear ion wave reaches the probe. Let us remind that the nonlinear ion wave has been found to travel down the density gradient with velocity $V_{down}\approx 4\times 10^5$ cm^{-3}, which is approximately twice the sound speed c_s. The energetic ion component, whose typical velocity is

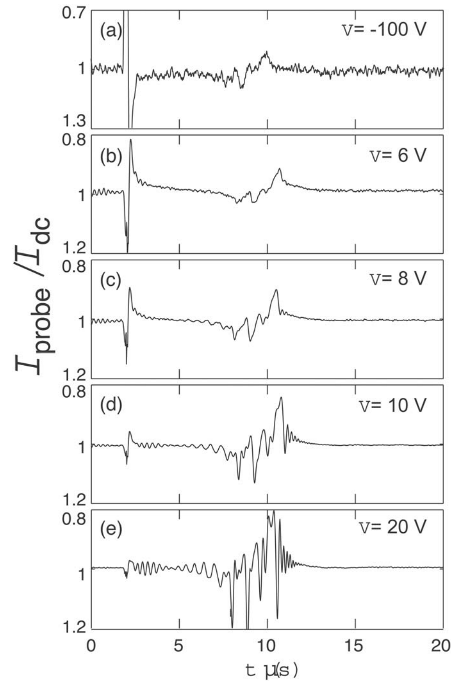

FIG. 6. Normalized probe currents at different biases. The instability occurs only at high positive probe biases [(d) and (e)], while at smaller biases [(a)–(c)] only the nonlinear ion wave is detected.

indicated in Fig. 8 as V_b, reaches the probe earlier than the ion wave ($V_b\approx 8\times 10^5$ cm^{-3} corresponds to 12 eV ions, compare with Fig. 2). Hence, we may suppose that the sheath instability is caused by the energetic ion component entering the sheath with velocities $V_b\sim(3-5)c_s$.

The amplitude of the oscillations in the electron saturation current depends on the load resistance R in the probe scheme (Fig. 9). Note that for all the measurements in Fig. 9, the load resistances are significantly smaller than the ratio V_{probe}/I_{dc}, hence the probe potential does not vary for different oscillograms in Fig. 9. One may observe that the amplitude of low-frequency oscillations does not depend on the load resistance at $R<100\ \Omega$ and they disappear at

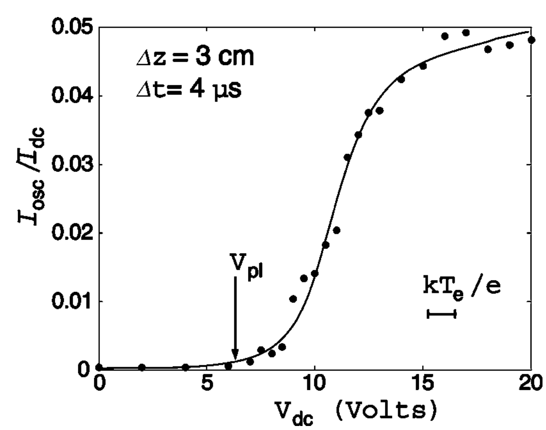

FIG. 7. Relative instability amplitude vs dc bias voltage showing that the instability occurs only when the probe is biased positively with respect to the plasma. The probe is located $\Delta z=3$ cm below the resonant region. The instability amplitude is measured at $\Delta t=4\ \mu$s after finishing the microwave pulse. The plasma potential and electron temperature are indicated.

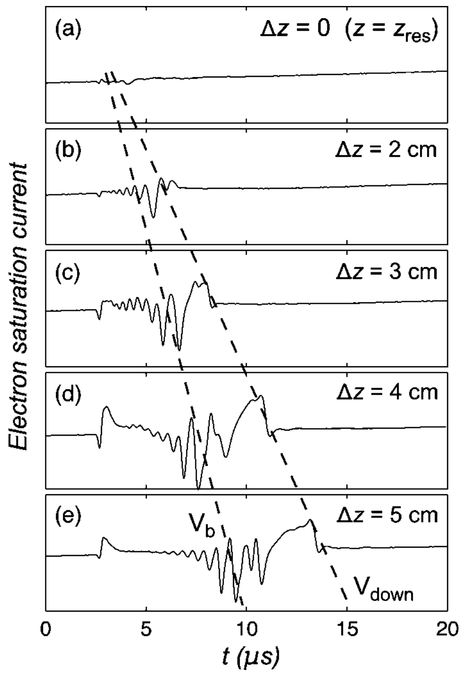

FIG. 8. Electron saturation current ($V=50$ V) at different distances from the resonance absorption region showing that the instability is driven by the energetic ion flux produced by the resonant absorption process.

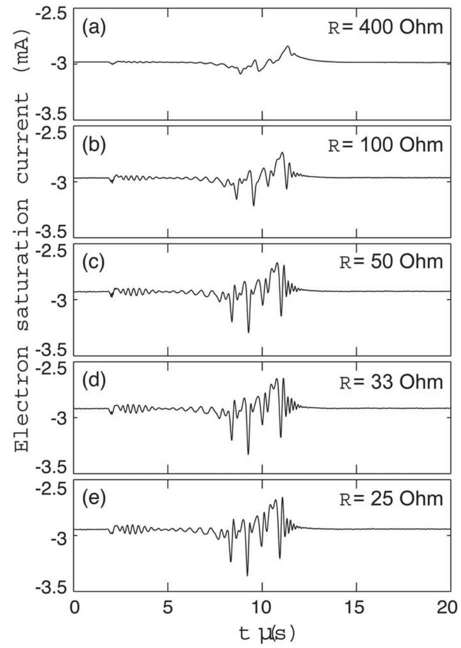

FIG. 9. The electron saturation current at different load resistances R. One may observe that the instability is detected only at $R<100\ \Omega$, while higher R quench the instability.

$R>100\ \Omega$. These results prove again that the observed oscillations are not due to the oscillating plasma density.

Summarizing the above measurements, the observed low-frequency oscillations of the electron saturation current do not represent plasma density perturbations, but are due to the instability of the electron-rich sheath driven by the energetic ion-beam component.

C. Model of the instability

The instability has been observed for a plane probe, when the unperturbed sheath thickness ($r_s \approx 5 \times \lambda_D \approx 0.2$ mm, where λ_D is the Debye length) is very small as compared with the probe diameter, $D=2$ mm. Thus, to interpret correctly the oscillations observed in the electron saturation current, one should consider planar oscillations in the electron-rich sheath under the influence of energetic ions entering the sheath area. We suggest a simple physical model, which may explain how a pulsed ion beam may cause the oscillations in the electron-rich sheath of an electrode. Consider a positively biased plane probe immersed into a plasma with a pulsed ion beam. If the probe potential U_0 is greater than the ion-beam energy U_b, the ion-beam front is reflected inside the electron-rich sheath. Near the reflection point the density of beam ions increases by many times and diminishes, consequently, the total negative space charge of the sheath. As a result, an overshoot of the electron saturation current occurs due to the fact that the plasma ions do not evacuate instantaneously (recall that $\nu_b \gg c_s$, from the present experimental data). The duration of the overshoot corresponds to the time ($\tau_s \approx r_s / c_s \approx 0.15\ \mu$s), which it takes the plasma ions to move across the sheath region ($r_s \approx 5\lambda_D \approx 0.2$ mm) with the sound speed ($c_s \approx 1.5 \times 10^5$ cm/s). During this time interval, the positive probe potential penetrates strongly into the plasma and, in turn, influences the ion beam: while the beam front propagates toward the probe through a potential-free plasma, the subsequent part of the beam propagates through decelerating potential. Hence, the ion-beam disruption occurs due to the time-of-flight effect and the beam density inside the sheath decreases leading the sheath back to its initial, unperturbed state. If the beam disruption time is long enough (i.e., of the order of τ_s or longer), the sheath will return to the unperturbed state and all the above processes will continue for the subsequent part of the beam.

A detailed analysis of the described ion-beam-sheath interaction implies a rather complicated dynamics of plasma particles, which require further theoretical and numerical investigations. Let us stress that the instability has been observed in a rather complicated experimental situation, when different plasma disturbances may occur simultaneously. Thus, to identify exactly the nature of the instability, further experiments should be performed using other approaches that would simplify the experimental conditions. For example, using other ion-beam sources, we may perform an experiment in a quiescent, uniform plasma penetrated by a controllable, monoenergetic ion beam.

The above model deals with the planar sheath geometry. However, it has been shown[33,34] that the reflection of energetic ions inside the sheath causes significant sheath expansion, such that the sheath thickness may increase considerably. In such situation, if the plane probe is relatively small, the geometry of the expanded sheath may change to a spherical one, which may cause additional effects, such as reflection of energetic ion sideways, etc. In order to show that the observed oscillations are not due to the modification of the sheath geometry, the measurements have been performed us-

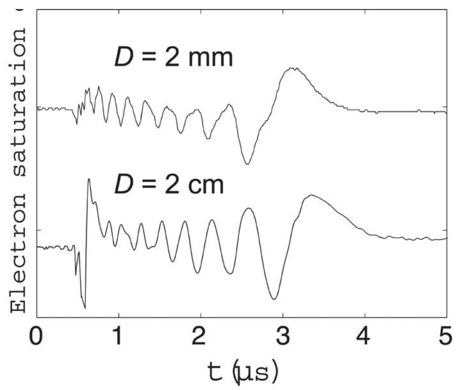

FIG. 10. The instability observed at two probe diameters showing that the model of plain sheath expansion should be used to explain the nature of the instability.

ing a large plane probe 2 cm in diameter. In this case, even strong sheath expansion would not modify the sheath geometry. Figure 10 represents two typical oscillograms of the electron saturation current obtained for the probes with diameters $D=2$ mm and 2 cm, respectively. One may see that the characteristics of the instability (period and relative amplitude) are practically the same in both cases. These measurements support the model of planar sheath expansion.

The proposed model of the instability deals with the violation of the charge balance in the sheath. To support this point, the following measurements have been performed. If the sheath reaction to the entrance of the beam front is so fast that the charge balance in the sheath is not violated, then no beam disruption occurs and the instability should not develop. In pure argon plasma such a fast sheath reaction cannot be realized, since $v_b \gg c_s$. In order to make the sheath reaction faster, the experiments were performed in the mixture of argon and hydrogen. If the density of light ions on the sheath-plasma boundary is higher than the beam density, then the motion of the light component is sufficient to neutralize the additional space charge which occurs when the beam front enters the sheath. Figure 11 displays the electron saturation current at different hydrogen pressures. One may see that the addition of about 10% of hydrogen [Figs. 11(c) and 11(d)] quenches the instability, though plasma parameters do not vary noticeably.

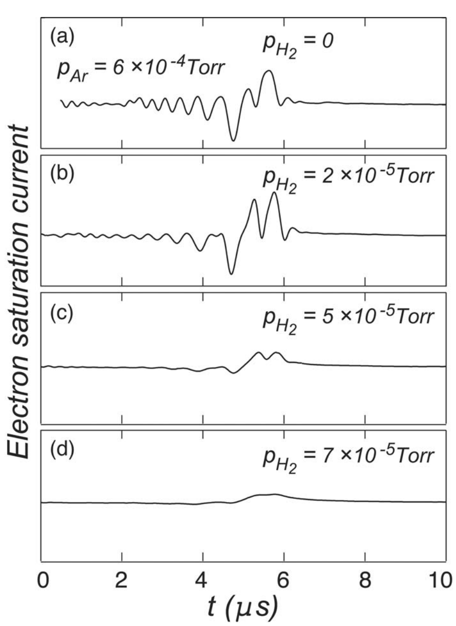

FIG. 11. The low-frequency instability measured in a pure argon plasma (a) and in mixtures of argon and hydrogen [(b)–(d)] at different pressures of hydrogen. The instability is suppressed by the movement of light ions across the sheath.

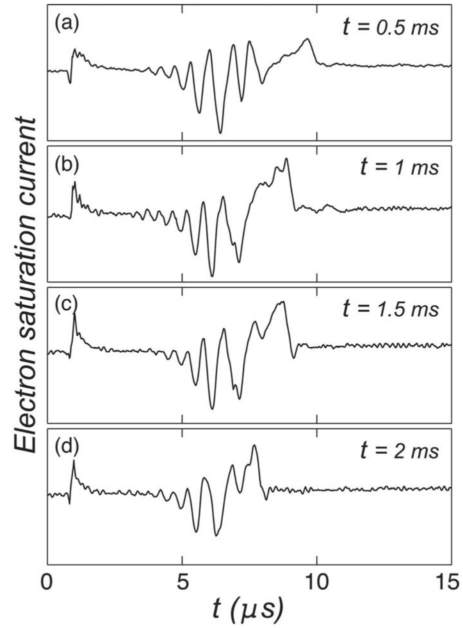

FIG. 12. The low-frequency instability measured in the afterglow plasma at different afterglow times t. The instability is observed even in late afterglow [(b)–(d)], although the plasma is isothermic ($kT_e \approx kT_i \approx 0.3$ eV) in this case.

To interpret the last results correctly, one needs further clarifications connected with the fact that the addition of light ions causes strong Landau damping of the ion acoustic mode. In order to show that the observed instability is not influenced by ion Landau damping, we performed the measurements of the electron saturation current in the afterglow mode, when $kT_e \rightarrow kT_i$. In these measurements, we produced more dense plasma in the discharge ($4\times 10^{11}-10^{12}$ cm^{-3}) and the microwave pulse was triggered, when plasma density decreased to 10^{11} cm^{-3} in the afterglow. Oscillograms of the electron saturation current in the afterglow mode are presented in Fig. 12. One may clearly see that the instability is not influenced by ion Landau damping, since the oscillations in the electron saturation current are observed even in the late afterglow [Figs. 12(b)–12(d)], when $kT_e \approx kT_i$. These measurements prove that the quenching of the instability observed in the H^+-Ar^+ plasma (Fig. 11) is not due to Landau damping, but due to fast movements of light ions across the sheath. Moreover, the fact that the oscillations are not suppressed by ion Landau damping denies their wave nature.

IV. DISCUSSION AND CONCLUSIONS

A new kind of low-frequency sheath instability presented in our previous paper[26] is reported in more detail.

New experimental results clarify the nature of the instability and support its qualitative model.

The instability with its characteristic frequency lower than the ion plasma frequency has been found in a laboratory plasma containing an accelerated ion component. The instability is observed in the sheath of a positively biased electrode, when its surface is irradiated by the energetic particles produced through the resonant absorption of a short microwave pulse. A qualitative model of the instability is proposed to explain the occurrence of the sheath instability when an electron-rich sheath is irradiated by a pulsed ion beam. According to the model, the instability occurs if the ion beam is reflected inside the sheath, which violates the charge balance and makes the electric field of the electrode to penetrate into the plasma volume. Consequent disruption of the ion beam produces an oscillation in the electron saturation current.

The proposed qualitative model needs to be supported by additional theoretical and experimental investigations. For example, the contribution of the accelerated electron component, as well as the influence of the sheath geometry to the observed instability should be clarified. The experiments using other ion-beam sources with controllable beam density and energy should also shed light on the physical processes in the sheath, when the latter interacts with a pulsed ion beam.

The observed phenomena can occur both in space and laboratory plasmas with non-Maxwellian ion distributions and could contribute to the particle collection process in plasma discharges and active space plasma experiments (including beam injection, electrodynamic tethers, or rf ionospheric heating). Let us also notice that the observed instability could be used as a sensitive diagnostic of the energetic ion component in a plasma. Indeed, the oscillations in the electron saturation current produced by an ion beam can be detected easier than the ion beam itself.

ACKNOWLEDGMENTS

A part of the present work was supported by a Grant-in-Aid for Scientific Research from the Ministry of Education, Science, Sports, and Culture, Japan. One of the authors (M.S.) was supported by Satellite Venture Business Laboratory of Utsunomiya University and by grants of the President of Russian Federation for Young Candidates of Science (Grant No. MK–4355.2004.2), Russian Foundation for Basic Research (Grant No. 04–02–17105) and Russian Science Support Foundation.

[1] I. Langmuir and H. M. Mott-Smith, Phys. Rev. **28**, 727 (1926).
[2] I. D. Kaganovich, Phys. Rev. Lett. **89**, 265006 (2002).
[3] M. A. Liebermann, IEEE Trans. Plasma Sci. **16**, 638 (1988).
[4] Y. P. Bliokh, J. Felsteiner, and Y. Z. Slutsker, Europhys. Lett. **46**, 735 (1999).
[5] Y. P. Bliokh, J. Felsteiner, Y. Z. Slutsker, and P. M. Vaisberg, Phys. Plasmas **9**, 3311 (2002).
[6] R. L. Stenzel, Phys. Rev. Lett. **60**, 704 (1988).
[7] R. L. Stenzel, Phys. Fluids B **1**, 1369 (1989).
[8] M. C. Griskey and R. L. Stenzel, Phys. Rev. Lett. **82**, 556 (1999).
[9] D. Arbel, Z. Bar-Lev, J. Felsteiner, A. Rosenberg, and Y. Z. Slutsker, Phys. Rev. Lett. **71**, 2919 (1993).
[10] Y. Nakamura and S. Sato, Phys. Plasmas **10**, 900 (2003).
[11] F. F. Chen, *Plasma Diagnostic Techniques*, Chap. 4, pp. 113–200.
[12] D. G. Bills, R. B. Holt, and B. T. McClure, J. Appl. Phys. **33**, 29 (1962).
[13] K. Takayama, H. Ikegami, and S. Miyazaki, Phys. Rev. Lett. **5**, 238 (1960).
[14] V. A. Godyak, A. N. Ivanov, and A. A. Kuzovnikov, Sov. Phys. Tech. Phys. **37**, 1063 (1967).
[15] M. V. Nezlin, *Physics of Intense Beams in Plasmas* (IOP, Bristol, 1993).
[16] V. A. Godyak, Sov. J. Plasma Phys. **2**, 78 (1976).
[17] D. Arbel, Z. Bar-Lev, J. Felsteiner, A. Rosenberg, and Y. Z. Slutsker, Phys. Rev. Lett. **78**, 66 (1997).
[18] Y. P. Bliokh, J. Felsteiner, Y. Z. Slutsker, and P. M. Vaisberg, IEEE Trans. Plasma Sci. **29**, 895 (2001).
[19] A. V. Kostrov, A. I. Smirnov, M. V. Starodubtsev, and A. A. Shaykin, JETP Lett. **67**, 579 (1998).
[20] M. Dobrovolny and E. Melchioni, J. Geophys. Res. **98**, 13761 (1993).
[21] R. L. Stenzel and J. M. Urrutia, J. Geophys. Res. **95**, 6209 (1990).
[22] R. L. Stenzel and J. M. Urrutia, Phys. Plasmas **4**, 26 (1997).
[23] K. H. Wright, N. H. Stone, J. Sorensen, J. D. Winningham, and C. Gurgiolo, Geophys. Res. Lett. **25**, 417 (1998).
[24] L. Linson, J. Geophys. Res. **74**, 2368 (1969).
[25] L. Iess, C. Harvey, G. Vannaroni, J. P. Lebreton, M. Dobrowolny, R. Manning, P. Cerulli-Irelli, A. Onelli, and F. D. Venuto, Geophys. Res. Lett. **25**, 421 (1998).
[26] M. Starodubtsev, M. K. Al-Hassan, H. Ito, N. Yugami, and Y. Nishida, Phys. Rev. Lett. **92**, 045003 (2004).
[27] V. L. Ginzburg, *The Properties of Electromagnetic Waves in Plasmas* (Pergamon, New York, 1964).
[28] A. Y. Wong and R. L. Stenzel, Phys. Rev. Lett. **34**, 727 (1975).
[29] W. Gekelman, R. L. Stenzel, and N. Wild, J. Geophys. Res. **87**, 101 (1982).
[30] R. L. Stenzel, W. Gekelman, and N. Wild, J. Geophys. Res. **88**, 4793 (1983).
[31] R. L. Stenzel, Rev. Sci. Instrum. **47**, 603 (1976).
[32] R. L. Stenzel, Phys. Fluids B **1**, 2273 (1989b).
[33] Y. Nakamura, Y. Nomura, and R. Stenzel, J. Appl. Phys. **52**, 1197 (1981).
[34] R. Stenzel, M. Ooyama, and Y. Nakamura, Phys. Fluids **24**, 708 (1981).